




Surface sediment composition and depositional environments in tropical Lake Sentani, Papua Province, Indonesia

Sulung Nomosatryo · Rik Tjallingii ·
Cynthia Henny · Iwan Ridwansyah ·
Dirk Wagner · Sara Tomás · Jens Kallmeyer 

Received: 9 October 2020 / Accepted: 16 July 2022 / Published online: 5 August 2022
© The Author(s) 2022

Abstract Tropical Lake Sentani in the Indonesian Province Papua consists of four separate basins and is surrounded by a catchment with a very diverse geology. We characterized the surface sediment (upper 5 cm) of the lake's four sub-basins based on multivariate statistical analyses (principal component analysis, hierarchical clustering) of major element compositions obtained by X-ray fluorescence scanning. Three types of sediment are identified based on distinct compositional differences between rivers, shallow/proximal and deep/distal lake sediments. The

different sediment types are mainly characterized by the correlation of elements associated with redox processes (S, Mn, Fe), carbonates (Ca), and detrital input (Ti, Al, Si, K) derived by river discharge. The relatively coarse-grained river sediments mainly derive from the mafic catchment geology and contribution of the limestone catchment geology is only limited. Correlation of redox sensitive and detrital elements are used to reveal oxidation conditions, and indicate oxic conditions in river samples and reducing conditions for lake sediments. Organic carbon (TOC) generally correlates with redox sensitive elements, although a correlation between TOC and individual elements change strongly between the three sediment types. Pyrite is the quantitatively dominant reduced sulfur mineral, monosulfides only reach appreciable concentrations in samples from rivers draining mafic and ultramafic catchments. Our study shows large spatial heterogeneity within the lake's sub-basins that is mainly caused by catchment geology and topography, river runoff as well as the bathymetry and the depth of the oxycline. We show that knowledge about lateral heterogeneity is crucial for understanding the geochemical and sedimentological variations recorded by these sediments. The highly variable conditions make Lake Sentani a natural laboratory, with its different sub-basins representing different depositional environments under identical tropical climate conditions.

Supplementary Information The online version contains supplementary material available at <https://doi.org/10.1007/s10933-022-00259-4>.

S. Nomosatryo · D. Wagner · J. Kallmeyer (✉)
Section Geomicrobiology, GFZ German Research Centre
for Geosciences, 14473 Potsdam, Germany
e-mail: kallm@gfz-potsdam.de

S. Nomosatryo · C. Henny · I. Ridwansyah
Research Center for Limnology and Water Resources,
National Research and Innovation Agency (BRIN),
Republic of Indonesia, Cibinong 16911, Jawa Barat,
Indonesia

R. Tjallingii
Section Climate Dynamics and Landscape Evolution, GFZ
German Research Centre for Geosciences, 14473 Potsdam,
Germany

D. Wagner · S. Tomás
Institute of Geosciences, University of Potsdam, Potsdam,
Germany

Keywords Tropical lake · Lacustrine sediment · XRF analysis · Multivariate statistics

Introduction

Chemical composition of lacustrine sediments is controlled by biological, chemical, and physical processes both within the lake and during sediment transport to the lake. In tropical regions with high precipitation, particulate and dissolved compounds are transported into the lake mostly by rivers (Stallard and Edmond 1983). In these regions, strong chemical weathering of bedrock material and rapid soil formation alters erosion products that are transported by streams and rivers and accumulate in lacustrine deposits. High temperatures and, at least during some parts of the year, high precipitation rates, lead to strong chemical weathering in the catchment, creating a high flux of suspended sediment and dissolved compounds from the catchment to the lake (Crowe et al. 2008; Liu et al. 2012). In aquatic environments, biological activity and the production of organic matter play a prominent role on the level of oxygenation in the water column and at the sediment–water interface (Santschi et al. 1990). Degradation of organic matter by heterotrophic microorganisms is the main consumer of dissolved oxygen (Holmer and Storkholm 2001). After oxygen has been depleted, compounds like metal (mostly Fe and Mn) oxides, nitrate or sulphate are being used as electron acceptors in the anaerobic degradation of organic matter (Froehlich et al. 1979). Heterotrophic degradation of organic matter, particularly with metals as electron acceptors, plays a dominant role on diagenetic alteration of lacustrine sediments (Capone and Kiene 1988). For example, solid ferric (oxyhydr)oxides can enter the lake either as detrital minerals or are formed in the water column under oxidizing conditions (Zeg-eye et al. 2012; Vuillemin et al. 2019). Upon depletion of electron acceptors with a higher energy yield, i.e. oxygen, nitrate, Mn^{4+} (Froehlich et al. 1979), these minerals can be reduced, producing dissolved Fe(II) which might diffuse upward and become oxidized again, or form ferrous minerals (Fredrickson et al. 1998; Vuillemin et al. 2019, 2020; Bauer et al. 2020). Even in highly oligotrophic systems with low organic carbon concentrations, anaerobic processes dominate sedimentary mineral transformation, as oxygen

only penetrates a few mm into the sediment (Corzo et al. 2018). Hence, sediments in tropical lakes are influenced by chemical weathering of bedrock in the catchment, fluvial transport, and alteration in the water column as well as diagenesis after deposition (Hasberg et al. 2019).

Despite all the chemical variations caused by a number of conditions and processes both in the catchment and the water column, the “finger print” of the source rock, i.e. its primary chemical signature is still at least partly visible in surficial lacustrine sediment. Elemental and mineralogical compositions of near-surface sediment provide detailed information on the distribution of the dominant sediment sources and the main depositional environments in a lake system. In addition, detailed characterization of depositional environments can provide fundamental information for the interpretation of sediment cores that archive long time series of depositional changes (Last and Smol 2001).

Most limnological studies are carried out in temperate lakes, whereas the special characteristics of lacustrine sediment in tropical lakes are still largely unknown (Escobar et al. 2020). The most important difference between temperate and tropical lakes are the small seasonal temperature fluctuations in the latter, leading to an often more stable temperature gradient in the water column that is not disturbed by changing surface water temperatures. However, even subtle temperature fluctuations in combination with increased evaporation during the dry season can lead to sufficient cooling to allow overturning of the water (Lewis 1987).

The main annual climatic variation is precipitation with one or two wet and dry seasons (Boehrer and Schultze 2008; Katsev et al. 2017). Therefore, many large tropical lakes like Malawi, Tanganyika and Matano are meromictic (Katsev et al. 2017), i.e. the water column is permanently stratified with a well-mixed oxic surface layer (epilimnion) and a denser anoxic deep layer (monimolimnion) (Crowe et al. 2008; Roland et al. 2017; De Crop and Verschuren 2019). Smaller lakes where the fetch across which the wind can blow and mix the water is small compared to the maximum water depth, can be meromictic as well. However, according to Schmid’s lake stability formula, deep but small lakes show only weak stratification (Hutchinson 1957). Irrespective of the size and maximum depth of a lake, stable stratification and

resulting meromixis has profound implications on the biogeochemistry of these lakes (Katsev et al. 2017).

Lacustrine sediments are often used for paleoclimate reconstructions, where long sediment cores are retrieved to obtain archives of past environmental conditions (Last and Smol 2001). However, as coring is logistically challenging and expensive, normally only very few sites that promise the longest and least disturbed sedimentary sequence are being cored. Especially for deep drilling projects the characterization of spatial heterogeneity has become an important aspect. In recent years several studies showed the importance of riverine input on lacustrine sediment and the spatial variability of sediment distribution within a single basin in several tropical and temperate lakes, e.g. Lake Turkana (Yuretich 1979), Lake Ohrid (Vogel et al. 2010), Lake Donggi Cona (Dietze et al. 2012), Lake El'gygytyn (Wennrich et al. 2013), Laguna Medina (van 't Hoff et al. 2016), or Lake Towuti (Hasberg et al. 2019; Morlock et al. 2019). Many of them showed that lateral heterogeneity can severely complicate reconstructions of paleoenvironmental conditions based on long sediment cores. In Lake Sentani Nomosatryo et al. (2021) sampled the water column and took sediment cores in the deepest part of each sub-basin. Their results showed that climatic and hydrological changes are recorded in sedimentary sequence. However, as this study only used one sampling location per basin, a differentiation between lateral variability and temporal climatic or hydrological changes was not possible.

In order to contribute to a better general understanding of the relationship between catchment geology and lacustrine sediment composition we studied the spatial distribution of sediment types in Lake Sentani in Papua Province, Indonesia (2° S, 140° E). A unique feature is the lake's shape, as it is divided into four sub-basins of which three are separated by shallow sills and one by a narrow natural channel (Fig. 1a) (Sadi 2014; Indrayani et al. 2015a). The catchment geology is highly diverse, ranging from carbonates over clastic sediments to igneous and metamorphic rocks, some with ultramafic composition (Suwarna and Noya 1995). The northern side of the lake is bounded by the Cyclops Mountains, the southern side has a relatively flat topography (Fig. 1b).

While the four basins share a common surface water chemistry, the basins differ in water column structure and bottom water chemistry. Moreover, each

sub-basin receives a distinct sediment input (Sadi 2014). Thus, this lake offers the chance to study the effects of different catchment lithologies and water column processes on lacustrine surface sediment under otherwise identical environmental conditions. Although the population around Lake Sentani is growing, and the lake faces increasing anthropogenic nutrient input (Kementerian Lingkungan Hidup Republik Indonesia 2011; Indrayani et al. 2015b), the area still has a relatively low level of urbanization despite its proximity to Jayapura, the capital of the province.

Study site

Lake Sentani is located near the capital city of Papua Province, Jayapura, at an elevation of 73 m asl (Fig. 1b). The lake is approximately 28 km long (East to West), 19 km wide (North to South), has a total surface area of 96.3 km² (Kementrian Lingkungan Hidup Republik Indonesia 2011) and a storage capacity of 4821.5 × 10⁶ m³ (Sartimbul et al. 2015). Lake Sentani consists of four sub-basins of which one is connected by a shallow natural channel (Simboro Channel), the other three are separated by shallow sills with a maximum depth of just 6 m (Fig. 1b). There are considerable differences in the maximum water depths of the four sub-basins, literature values range from 30 m (Sadi 2014) to 70 m (Indrayani et al. 2015a). Our own depth soundings at every sampling location revealed maximum depths of 42, 12, 30 and 43 m, for sub-basins 1 to 4, respectively. In a recent study, Nomosatryo et al. (2021) presented physico-chemical properties of the water column, measured at or close to the deepest parts of each basin. In short, the upper 10 m of the water column in all four basins is well mixed, below this depth dissolved oxygen (DO) decreases more or less rapidly and becomes fully depleted in sub-basins 1 and 4, in sub-basin 3 DO just reaches depletion at the sediment–water interface, and shallow sub-basin 2 remains fully oxygenated. Surface water temperatures in all four sub-basins are between 31 and 32 °C, bottom temperatures are around 29° C except for sub-basin 2, where temperatures remain above 30 °C (Fig. 2).

The lake has a catchment area of about 600 km² and is bounded by the Cyclops Mountains to the north (Tappin 2007) and lowlands to the south. The highest peak of the Cyclops Mountains is Merahriboh, reaching

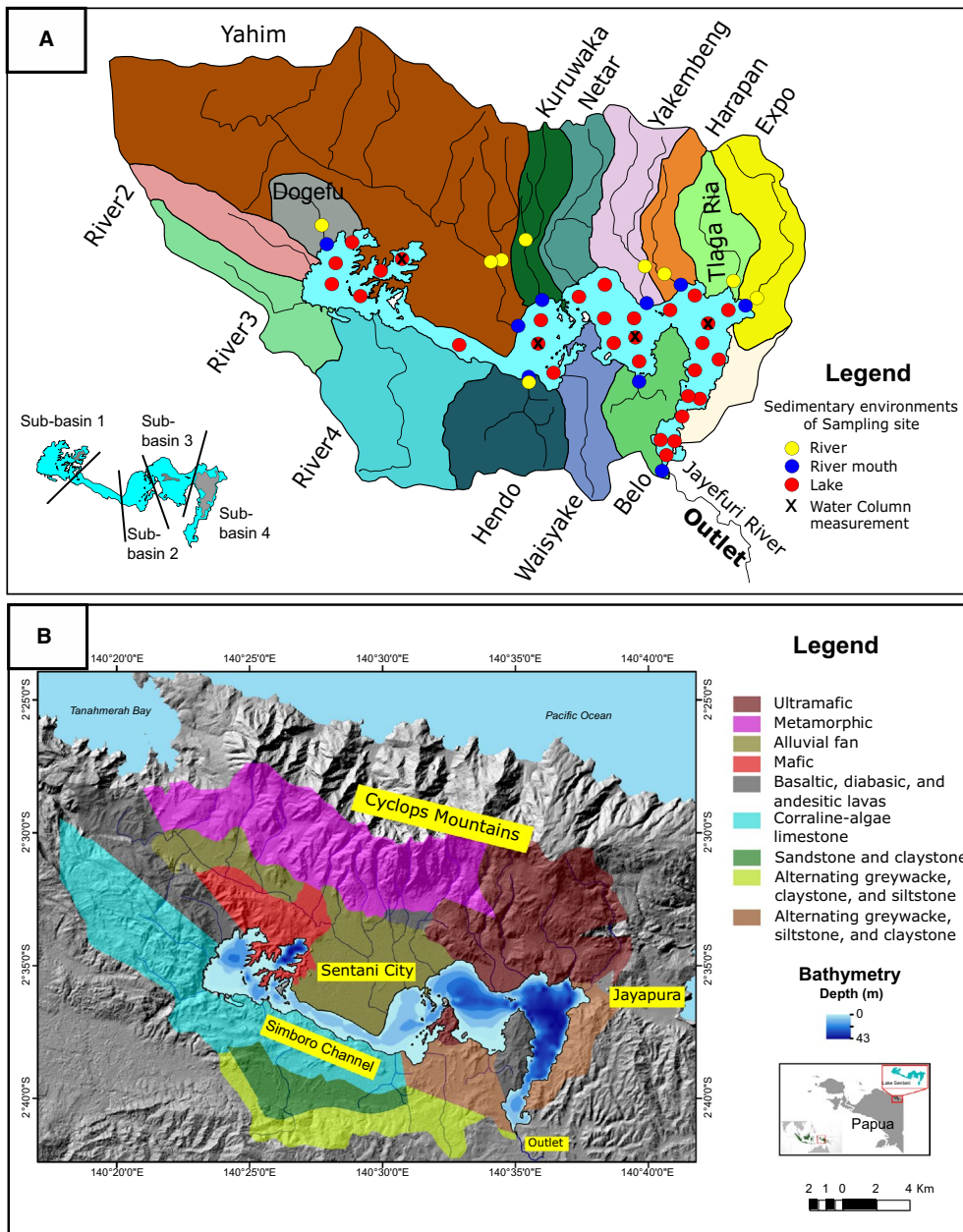


Fig. 1 Lake location and Setting. **A** Sampling sites and the Sub-catchments in Lake Sentani (digitized and modified after Sartimbul et al. (2015)). The circles indicate sampling sites in rivers (yellow), river mouths (blue) and lake (red). **B** Map of Lake Sentani and its surrounding watershed. Catchment

lithology is indicated by different colours. The lithology of Lake Sentani’s catchment is modified after Suwarna and Noya (1995). The low resolution bathymetric map is modified after Sadi (2014)

an elevation of 3200 m asl (Husein et al. 2018). The north side of the lake is dominated by volcanic breccia, mafic, ultramafic rocks and alluvial deposits, whereas the southern part of the lake is mainly characterized by a wide range of mainly sedimentary rocks comprised of various types of carbonates, siliciclastic sediments with some basaltic areas (Fig. 1b) (Suwarna and Noya 1995). At least sixteen rivers drain into the lake (Bungkang et al. 2014; Handoko et al. 2014). Yahim, the lake's largest sub-catchment is located on its northern side and covers almost 38% of the total catchment (Table 1). Twelve rivers come from the Cyclops Mountains in the north and four rivers originate from the lowlands in the south (Fig. 1). The Doyo River in the Yahim sub-catchment is the biggest single source of water to the lake with an average discharge of $19 \text{ m}^3 \text{ s}^{-1}$ (Table 1, Handoko et al. 2014). With the exception of the Warno River (discharge rate $5.5 \text{ m}^3 \text{ s}^{-1}$), which drains the Kuruwaka catchment immediately east of the Yahim catchment, all other rivers have discharge rates of $< 1 \text{ m}^3 \text{ s}^{-1}$. The Jayafuri (Jayefuri) River, located in the southeastern tip of the easternmost basin, is the only outlet (Handoko et al. 2014; Kementerian Lingkungan Hidup Republik Indonesia 2011). Discharge rate of the outflow at Jayafuri river is $15 \text{ m}^3 \text{ s}^{-1}$ (Handoko et al. 2014). The retention time of water in the lake is 510 days (Sadi 2014). Many catchment areas and rivers are known under different names (Table 1), but we will refer to the names of the sub-catchments (Fig. 1a, Sartimbul et al. 2015).

The average annual precipitation at Lake Sentani is $1691 \text{ mm year}^{-1}$ (Sartimbul et al. 2015). Highest precipitation occurs in March with an average of $206 \text{ mm month}^{-1}$; July has the lowest precipitation with 95 mm month^{-1} . Air temperature around Lake Sentani ranges between 23.6 and $32.2 \text{ }^\circ\text{C}$, the water temperature ranges between 29.3 and $30.4 \text{ }^\circ\text{C}$ (Sadi 2014).

Most of the catchment of Lake Sentani is dominated by natural vegetation (forests, grasslands) and agricultural areas with mainly sago plants (Kementerian Lingkungan Hidup Republik Indonesia 2011). Due to the mostly dense plant cover and the high precipitation, aeolian transport of sediment is negligible and we assume the sediments in and around the lake to be mostly fluvial or lacustrine, as in many tropical settings (Stallard 1998), however we cannot fully exclude other processes like mass wasting or

slumping, potentially triggered by the frequent earthquakes in the area (Mantiri 2016).

Materials and methods

Sediment sampling

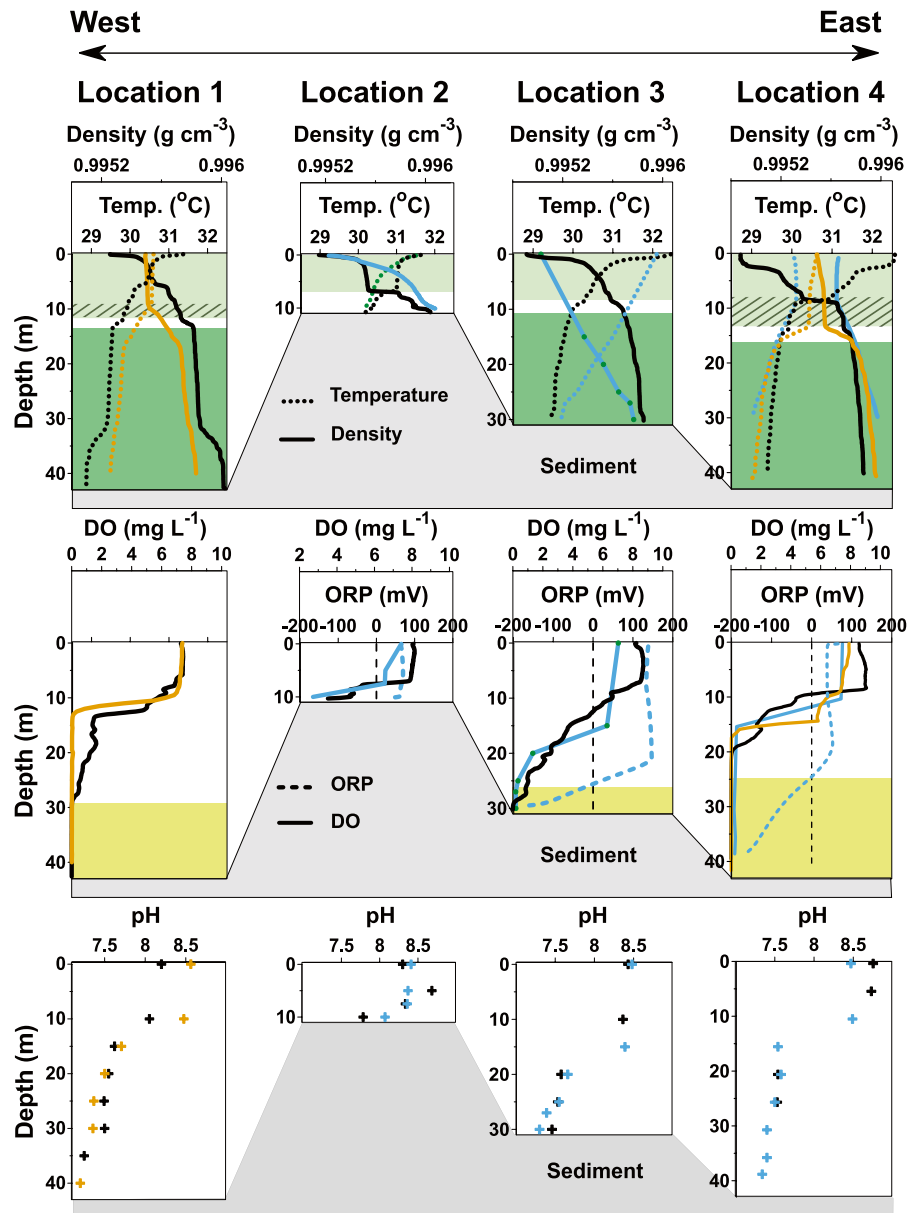
We collected surface sediment samples from 32 stations in the lake from water depths between 4 and 43 m, 8 samples from river mouths from water depths less than 4 m and 9 samples from rivers (Fig. 1a, ESM1). Sampling positions were determined by hand-held Global Position system (Garmin eTrex 10) and water depths determined by an echosounder (Garmin 42DV). Sampling was conducted using a short gravity corer, retrieving cores of up to 20 cm length, diameter 7 cm. Great care was taken to retrieve cores with an undisturbed sediment–water interface (SWI). Material was sampled from the upper 5 cm and each sediment sample was packed into a gas-tight aluminium foil bag and heat sealed. Due to the unavailability of nitrogen gas we tried to squeeze out as much air as possible, but some oxidation during storage and transport cannot be ruled out. Upon arrival in the home lab the sediment samples were freeze-dried and ground to completely pass a $63 \mu\text{m}$ -mesh sieve before analysis.

X-Ray Fluorescence (XRF) scanning and data analysis

About 4 g of freeze-dried sediment powder was loosely packed in sampling cups (ca 2 cm high, \emptyset 2 cm) and covered with a XRF transparent foil. Analysis of elemental sediment compositions was performed on these samples using an ITRAX XRF core scanner with a Cr X-ray source (operated at 30kv, 55 mA, 10 s).

XRF scanning analysis does not provide quantitative results but element intensities in counts per second. Relative element concentrations are provided by log-ratios of element intensities, which are free of physical and matrix effects (Weltje and Tjallingii 2008; Weltje et al. 2015). In addition, log-ratio-transformed intensities allow meaningful application of multivariate statistical analysis to characterize sediment compositions (Weltje et al. 2015).

Fig. 2 Water column profiles of density, temperature, dissolved oxygen (DO), oxidation–reduction potential (ORP), and pH of the four sampling locations in Lake Sentani (Fig. 1b). Measurements were taken in April (black) and November (green) 2016 and January (red) 2018. The profiles show a clear thermal stratification with a well-mixed epilimnion extending to about 10 m water depth (light green shading) and a denser hypolimnion below about 15–20 m (dark green shading), depending on the basin and time of measurement. Diagonal line pattern indicates the fluctuations of epilimnion boundary. Negative ORP values characterize the monimolimnion (yellow shading) with reducing conditions



Normalized relative concentrations are expressed by standardizing (Z-score) the log-transformed data.

TOC analysis

The concentration of TOC was determined by combusting between 15 and 100 mg of samples at 580 °C in a Vario Max C analyzer (Elementar Analysensysteme GmbH). The limit of detection was 0.1 wt%. To allow comparison of these

quantitative data with the semiquantitative XRF data, the TOC data were also transformed and standardized.

Pyrite quantification

For quantification of pyrite (FeS_2) and other sulfide minerals like FeS or MnS we performed a sequential cold chromium extraction (Kallmeyer et al. 2004). In short, 0.5–1 g of freeze-dried and finely ground sediment is placed in a distillation flask that is constantly

Table 1 Names and main characteristics of the rivers in Lake Sentani's catchment

Sub catchments	Bungakang et al. (2014), Fauzi et al. (2014)		Handoko et al. (2014)		
	Area (km ²)	Length of the river (m)	Slope (s)	Name of rivers	Discharge rate (m ³ s ⁻¹)
1	17	5010	0.0581	Dogefu/Kanda	0.24
2	25	6281	0.0718		n/a
3	29	6822	0.0475		n/a
4	64	14,099	0.053	Benali	0.14
Yahim	236	33,670	0.0424	Doyo Kemiri	19 0.36
Kuruwaka	23	12,165	0.1277	Belo Warno	0.62 5.47
Netar	25	12,243	0.1034	Flavouw	0.36
Yakembeng	33	13,061	0.0715	Yabawi	0.84
Harapan	19	9070	0.1072	Telaga maya	0.09
Expo	35	14,877	0.0664	Espo	0.23
Tiaga Ria	24	7769	0.0667		n/a
Hendo	40	5815	0.0253		n/a
Belo	24	6733	0.0148	Jembatan 2	0.55
Waisyake	25	10,598	0.0139		n/a

n/a no data available

flushed with nitrogen gas. Upon addition of 8 mL of 6 N HCl and constant stirring the acid volatile sulfur (AVS), mainly FeS and other monosulfides are dissolved and the liberated H₂S is transported by the flow of nitrogen into a trap filled with 7 ml of 5 wt% zinc acetate solution (ZnAc) where the H₂S precipitates as ZnS. After two hours the extraction is complete, the ZnAc trap is replaced by a fresh one and 16 ml of 1 M CrCl₂ solution is added to the flask through a valve to maintain strictly anoxic conditions in the distillation flask. The chromous chloride acts as a strong reductant and will promote breakdown of more crystalline reduced sulfur species like disulfides (Canfield et al. 1986; Luther 1987), of which pyrite is quantitatively most important. The H₂S that is liberated from the chromium reducible sulfur (CRS) is then also transported to the trap and precipitated as ZnS. The precipitates are centrifuged and the ZnAc-containing supernatant discarded as it interferes with downstream analyses. The ZnS pellet is resuspended in deionized water and sulfide is quantified photometrically using the methylene blue method (Cline 1969). Data are presented as the percentage of total reduced inorganic sulfur (TRIS) on total dry sediment, and the fraction of AVS on TRIS.

Smear slide analysis

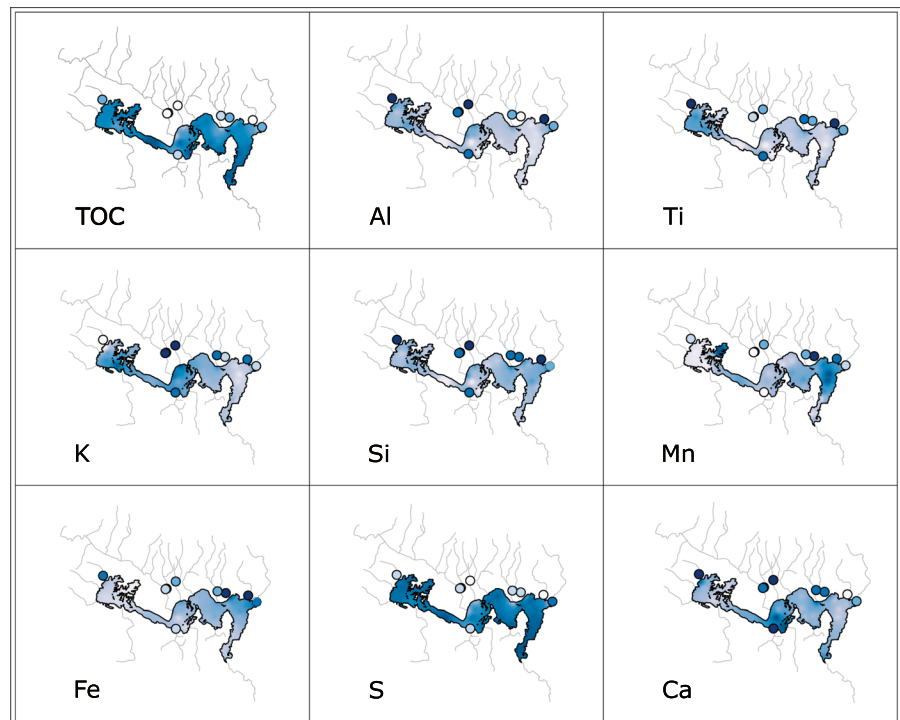
Smear-slide analyses were conducted on 24 selected samples, covering all four sub-basins and all sedimentary environments. A small amount of sediment (1–2 mm³) was picked from bulk wet sediment and dispersed in two drops of deionized water by swirling on a microscope slide to get a good particle separation and even distribution on the slide. The suspension was spread thinly to reach a just barely visible layer of sediment. The slide was dried on a hot plate at ~60° C. Once dry, the slide was covered by a cover slip mounted with two drops of low viscosity UV-glue (Ber-Fix 50–100, Ber-Fix Klebstoffprodukte Berlin, Germany). The glue was cured by exposing the slide to sunlight at room temperature until dry.

The 24 selected smear slides were studied for compositional characterization under a transmitted light microscope (Olympus BX 51). All components were characterized and their relative abundance visually estimated, with special emphasis on carbonate and mafic minerals, biogenic (diatoms and sponge spicules) and detrital silica content.

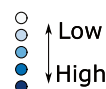
Grain-size analysis

Prior to analysis, organic matter was removed by adding 2.5 ml of 10 vol% H_2O_2 to bulk dry sediment aliquots of 0.5–0.7 g, followed by shaking for at least one week. If the reaction was still incomplete after one week, the treatment was repeated. Most samples were organic-free after one treatment, some organic-rich samples required a second round. The sediment residue was rinsed three times with 2.5 ml of de-ionized water followed by centrifugation and decantation of the supernatant. The sediment residue was then resuspended in 2.5 ml dispersion solution (35.7 g L^{-1} tetra-sodium diphosphate decahydrate, $\text{Na}_4\text{P}_2\text{O}_7 \cdot 10 \text{ H}_2\text{O}$) and placed in an overhead shaker for 24 h at 25 rpm. After complete dispersion, the entire volume of suspended sediment was measured with a Horiba LA-950 laser diffraction particle size distribution analyzer, providing 92 grain-size classes between 0.011 and 2500 μm . Each sample was measured 10 times with ultrasonic excitation.

Fig. 3 Relative distribution of major elements in the surface sediment of Lake Sentani and its rivers. Sampling sites in rivers are marked by blue circles. Graduated colors indicate relative element distribution (Z-score, see text for details). The same scale was used for river and lake samples



Relative distribution



Results

Sediment composition

Chemical analyses

The relative distribution maps were produced with the QGIS 2.18.11 free software, using the IDW spatial interpolation method. Relative distributions of TOC and 8 major elements (Al, Si, S, K, Ca, Ti, Mn, Fe) in Lake Sentani as well as its main tributary rivers reveal compositional differences within the lake sediment and its main sediment contributors (Fig. 3). Highest TOC concentrations of up to 27.9%_{dwt} (percent dry weight) are found in Simboro Channel between sub-basins 1 and 2 and at the lake's only outlet at the southern end of sub-basin 4. Generally, TOC concentrations are slightly higher in the southern parts of sub-basins 2 to 4. River samples have much lower TOC concentrations (average around 1.5%_{dwt})

compared to lake sediment samples (average around 11.5%_{dwt}).

Although relative concentrations differ, the distribution patterns of Al, Ti and K, all commonly associated with detrital minerals and known to be enriched in tropical soils, are generally similar (Fig. 3). Relative concentrations are highest in westernmost sub-basin 1 and decrease towards the east. River samples also reveal relatively high concentrations of the three elements with the exception of the Dogefu sub-catchment area at the north-western side of sub-basin 1, which shows low K and high Ti values. This pattern is surprising, given that the lake sediments of sub-basin 1 reveal an opposite pattern for these two elements (Fig. 3).

The distribution patterns of Mn and Fe are broadly similar with highest relative concentrations in the deep eastern sub-basin 4 and lower values in the three western sub-basins. However, there are subtle differences in the distribution pattern of these two elements within sub-basins 1 and 4. Throughout sub-basin 1 Fe shows low relative concentrations, whereas in the northeastern arm there is a strong enrichment in Mn. Iron values are high in the northern part of sub-basin 4, where the Tiaga Ria and Harapan sub-catchments drain into Lake Sentani. Sediment from the rivers draining these two catchments also reveal high relative Fe concentrations. Manganese concentrations rather follow bathymetry, with highest relative concentrations at the deepest part of sub-basin 4.

The distribution patterns of Si and S show that relative concentrations are evenly distributed throughout the lake (Fig. 3) whereas in river samples relative concentrations are much higher for Si and lower for S. Relative concentrations of Ca are highest in central sub-basin 2, where runoff from the sub-catchments Hendo and Waisyake enter the lake, both dominated by limestone of the Jayapura Formation, intercalated silt- & claystone and shale of the Makat Formation, and alluvial deposits. However, river samples reveal high relative Ca distribution in the Dogefu and Kuruwaka sub-catchments as well (Figs. 1a, 3) but the lake samples closest to these rivers are apparently not affected. Silica shows a relatively even distribution with only minor positive or negative relative distribution peaks (Fig. 3), however, the smear slide analyses show that the sources of silica vary considerably (Fig. 4a).

Smear slide analyses

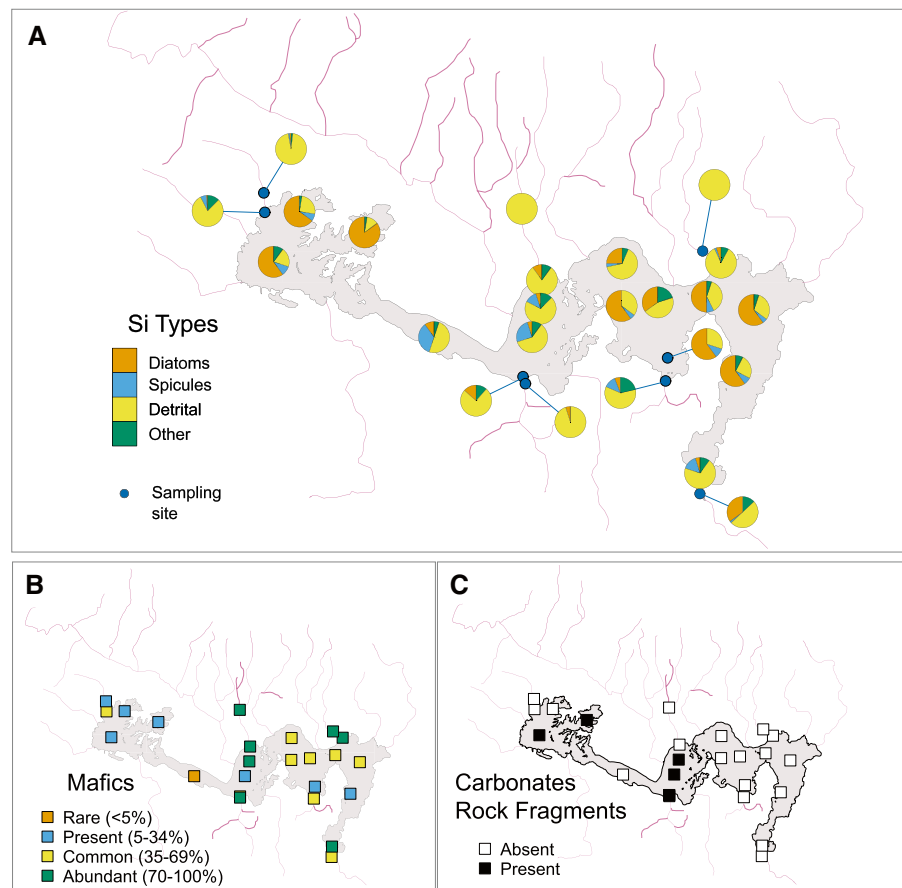
Smear slide analyses reveal the presence of diatoms and sponge spicules in almost all samples, together with detrital quartz grains (Fig. 4a). Other siliceous compounds like phytoliths are only found in some lake samples but never play a quantitatively significant role. Biogenic compounds are much more abundant in the two deepest sub-basins 1 and 4 and in the deeper parts of sub-basin 3, whereas detrital silica dominates the shallow sub-basins 2, the southern part of sub-basin 3, as well as the river samples. The only notable exception is the single sample in the Simboro channel that has the highest relative abundance of spicules of all samples, and only about 50% detrital silica (Fig. 4a, ESM1).

The smear slide analyses also confirm the dominance of the mafic and ultramafic geology on the sediment composition of the lake (Fig. 4b). With the exception of the single sample at Simboro channel where mafics were rare, they were present in all other samples. Highest abundances were found in samples from rivers and river mouths, mostly at the northern end of sub-basins 2 and 4, an area that is predominantly characterized by mafic and ultramafic catchment geology. In samples from sub-basin 1 mafic minerals are present but less abundant than in the other sub-basins. The distribution of carbonates reveals the close relationship between catchment geology and sediment composition (Fig. 4c). Samples closest to the limestone-dominated catchment located south west of the lake contain carbonates, whereas they were absent in all other samples. A notable exception is the presence of carbonate in a sample from the northeastern arm of sub-basin 1, which is entirely surrounded by mafic rocks.

Pyrite quantification

Pyrite and other reduced inorganic sulfur components could be detected in all samples with maximum concentrations of 5.4%_{dwt} (percent dry weight), although some had TRIS (Total Reduced Inorganic Sulfur) concentrations as low as 0.01%_{dwt} (Fig. 5a). Overall, chromium reducible sulfur (CRS) is the quantitatively dominant reduced inorganic sulfur species. As pyrite is the only CRS species detectable by X-Ray Diffraction in these samples (Fig. 5b), we assume that pyrite is in fact the dominant reduced inorganic sulfur

Fig. 4 Results of Si-speciation and proportions of mafic and carbonate rock fragments obtained from smear-slide analysis



species. Acid Volatile Sulfur (AVS, mostly monosulfides) accounts for less than 1% of TRIS in most samples. Concentrations of AVS exceeding 10% TRIS were found only in samples from rivers that drain the ultramafic catchment north of the lake as well as in samples from the corresponding river mouths.

Grain size distribution

There are clear geographic differences in the distribution of the different grain size classes (Fig. 6). Clay (1–4 μm particle size) accounts for up to 34% of the sediment in the southern parts of sub-basins 1 and 2 and the connecting Simboro channel. In the northern parts of these two sub-basins and elsewhere concentrations are much lower and usually below 10%. River samples show even lower clay contents in the low single-digit percent range. Silt (4–63 μm particle size) makes up the bulk of Lake

Sentani's sediment, accounting for up to 86% and shows an almost opposite distribution pattern to clay. Silt concentrations are lower in the southern parts of sub-basins 1 and 2 and the Simboro Channel, but with lowest concentrations still exceeding 35%. Silt content in river sediment varies over almost the entire concentration range with no visible pattern. Sand only makes up a comparatively small fraction of the lake sediment, concentrations are usually below 10%, higher values are only found around river mouths. Two samples from rivers draining the Yahim and Kuruwaka sub-catchments show high sand content of up to 52%.

Multivariate analysis of the chemical composition of the sediment

Statistical clustering allows identification of sediment samples with similar geochemical compositions. Here we use Ward's hierarchical clustering after z-scoring

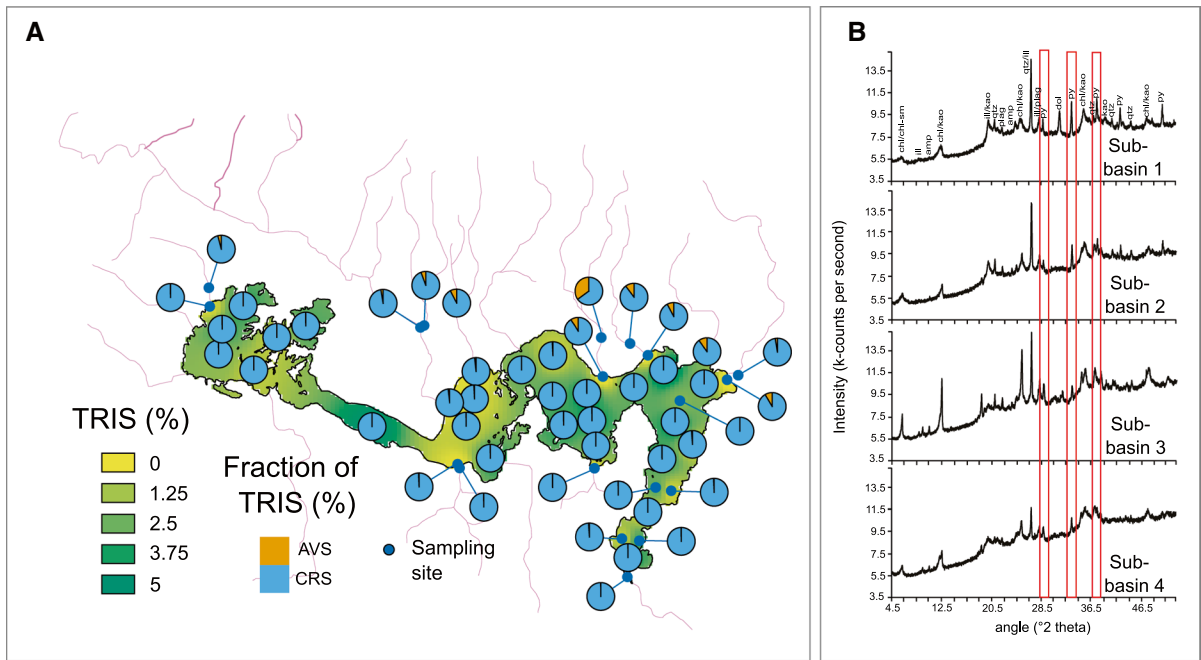


Fig. 5 Distribution of total reduced inorganic sulfur in Lake Sentani. Pie diagrams indicate in red the fraction of AVS (acid volatile sulfur, i.e. monosulfides) and in green CRS (chromium reducible sulfur, i.e. pyrite) among the Total Reduced Inorganic Sulfur (TRIS) pool at each sampling site. Total TRIS

concentration is provided by graduated colors. **B** X-Ray Diffractograms of representative samples from each sub-basin. Pyrite is the only identifiable mineral that contains reduced sulfur

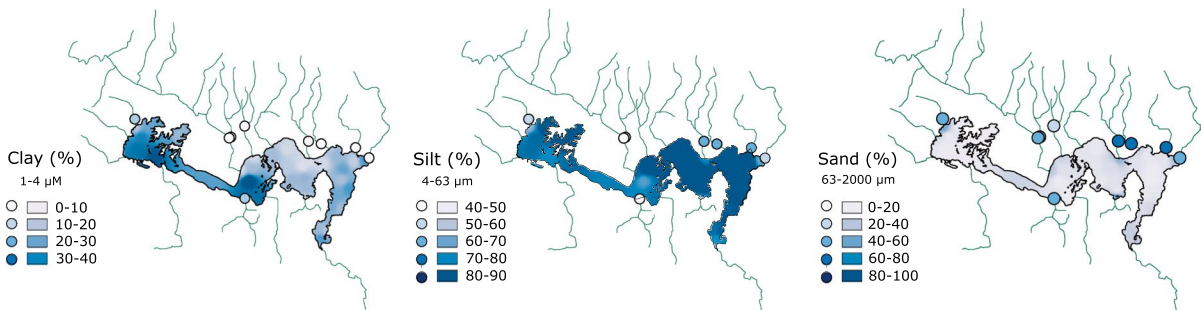


Fig. 6 Grain size distribution of Lake Sentani's surface sediment. For river samples the values are presented in circles

of the clr-transformed data of the major elements obtained by XRF scanning and TOC. Ward's hierarchical clustering of the geochemical composition was analyzed by using PAST3 (Hammer et al. 2001) and principal component analyses (PCA) was carried out with prcomp in the R statistical package 'composition'. A three-cluster-solution with an Euclidian linking distance of >2.5 was chosen as it explains the

largest differences in the dataset for the minimal number of clusters (ESM2).

Element correlations of each cluster are explored using PCA biplots of PC 1 and 2 (Fig. 7a) that explain about 70% of the variance for all three clusters (C1=68.9%; C2=71.6%; C3=71.9%). The clusters mainly comprise river and river mouth samples (cluster C1), lake samples from mostly shallow and near-shore (proximal) locations (C2), and deeper

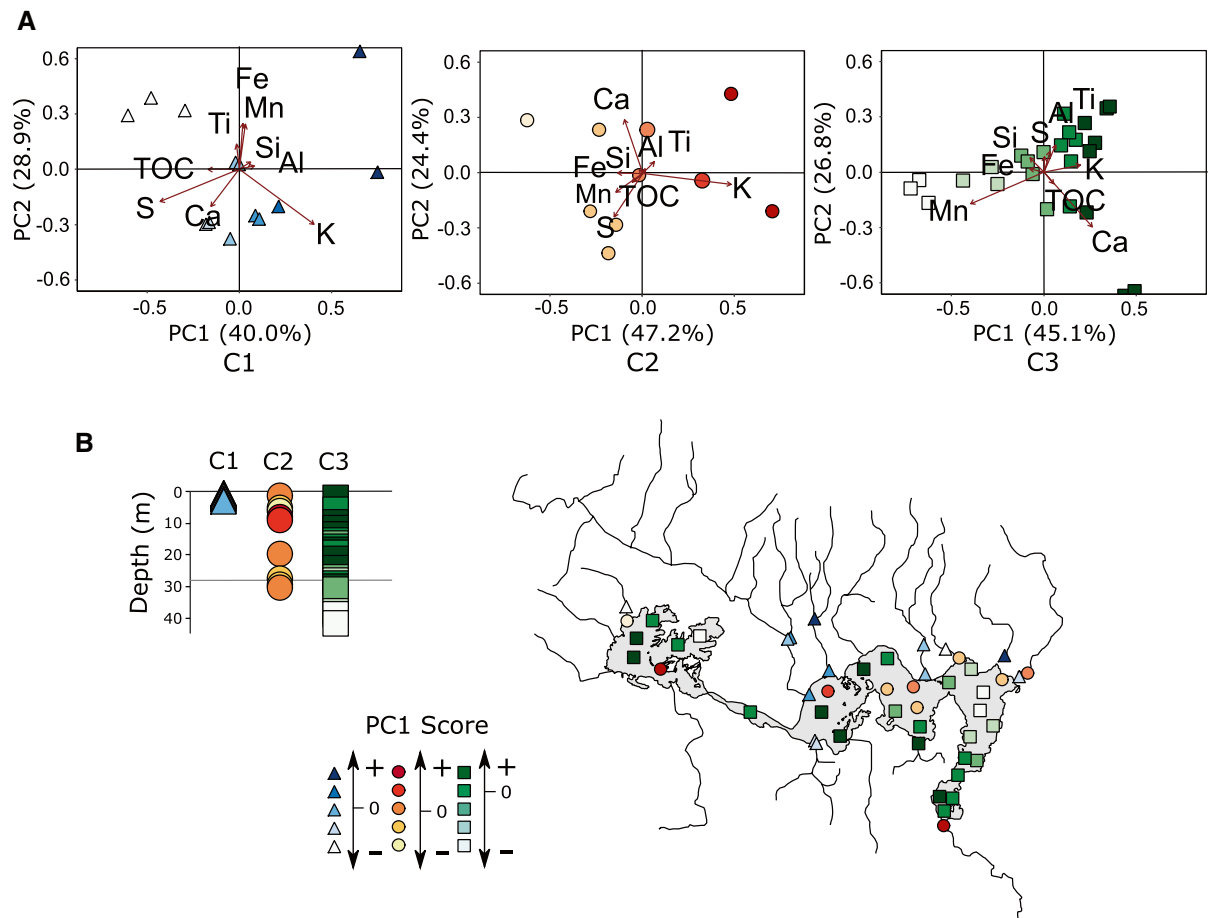


Fig. 7 Multivariate analyses including clustering of the relative elemental concentrations of the bulk sediment. **A** Ward's hierarchical clustering of relative elemental concentrations results in three main clusters with distinctly different correla-

tions. **B** Distribution of samples of the three different clusters, colors indicate their respective PC1 factor score. The inset shows the depth distribution of the samples of each cluster

or more distal lake locations (C3). The river cluster (C1) shows a clear separation between Ca and most of the detrital elements (Fig. 7a) associated with the southern limestones and northern mafic catchment geologies, respectively. Although TOC concentrations are only low in river samples, TOC and S are orientated in the same direction along PC1, indicating the positive correlation. However, the positive correlation between redox sensitive elements (Mn, Fe) and the inert element Ti, as indicated by the same direction along PC2 (Fig. 7a), suggests that degradation of organic matter and redox alteration of these sediments is neglectable.

Redox conditions seem to intensify for samples of the shallow/proximal lake cluster C2, as show a

positive correlation between TOC and the elements S, Mn and to a lesser extend Fe that all point in the same direction with respect to PC1. The deeper/distal lake samples of cluster C3 reveal a similar orientation of both elements Mn and Fe along PC1, suggesting that reduced conditions prevail in these sediments (Fig. 7a). Data distribution of cluster C3 reveals that the strongest redox conditions occur in the deepest part of the lake. The distribution of Ca (Fig. 3) is similar to the carbonate rock fragments (Fig. 4c) but deviates from the detrital elements Ti and K (Fig. 3), which is also apparent by the different directions/correlation of these elements (Fig. 7a). The similar direction of the detrital elements Ti, K and Al indicates positive correlation of these elements in clusters

C2 and C3 and association with sediments receiving input from catchments composed of siliciclastic rocks. In addition, river samples of C1 and lake samples of C2 and C3 reveal a different correlation between Si and detrital element Ti, K and Al, which is due to the abundance of diatoms and spicules in lake sediments (Fig. 4).

Most samples of cluster C2 are located above the oxycline and a few samples of sub-basin 3 are located around or just below, which is probably related to the less pronounced oxycline and stratification of this sub-basin (Fig. 2). The wide depth range of C3 shows that this cluster is more representative for lake sediments in general, ranging from oxic to anoxic. Within C1, highest PC1 factor scores are found in rivers in the north (Fig. 7b), lowest values in the south. For the PC1 values of C2 there is no apparent geographic distribution pattern or visible correlation with water depth. Cluster C3 encompasses lake samples from shallow to maximum depth, with most of the deep lake sediment samples located below the oxycline. The PC1 values decrease with water depth and indicate stronger reducing conditions with increasing the water depth.

Discussion

Distinct geochemical differences between rivers and lake sediments are found using statistical clustering that can identify samples with similar elemental compositions and provides a more detailed look into the different geochemical characteristics of the sediment (Fig. 7, ESM2). The three clusters reveal a clear compositional differentiation between river and river mouth samples (cluster C1), lake samples from mostly shallow and near-shore (proximal) locations (C2), and deeper and more distal lake locations (C3).

Rivers and river mouths represented by cluster C1 reveal a clear separation between Ca and most other elements that matches finding of carbonate rock fragments (Fig. 4c) and the special element distributions (Fig. 3). These distributions are associated with the contributions of different catchment geologies (Fig. 1). Moreover, the negative correlation between Ca and the elements Ti, Mn and Fe in cluster C1 (Fig. 7a) can be associated to the limestone catchment located south of the basin and the iron- and manganese-rich mafic and ultramafic

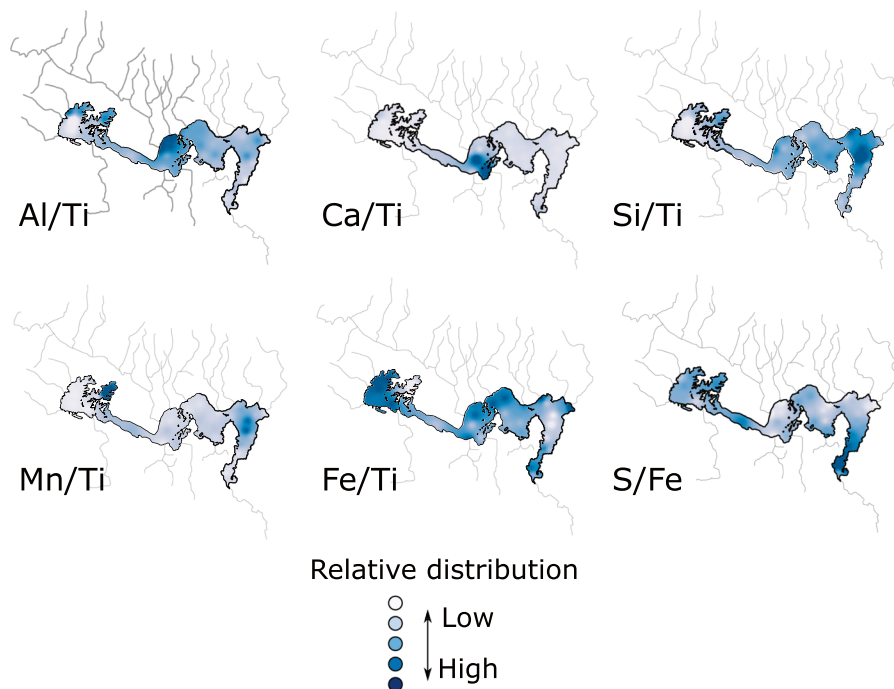
rocks in the Cycloop mountains in the north (Fig. 1a). The influence of diagenetic transformations (Raiswell and Canfield 2012) in the sediments of C1 is highly unlikely due to the low amounts of TOC (Fig. 3) and the positive correlation of Mn and Fe with the inert element Ti (Fig. 7a). However, diagenetic transformation of Mn and Fe due to changes in redox chemistry does influence the sediments of clusters C2 and C3, which is probably caused by anaerobic organic matter degradation processes in the anoxic sediment, even under conditions with oxygenated bottom waters. Under oxygen-limited or anoxic conditions anaerobic reduction process can take place not just in the sediment but also in the water column and at the sediment–water interface and no re-oxidation of reduced species through diffusion of oxygen from the water column or burial of oxidized minerals into the sediment can take place.

Multiple processes influence distribution patterns of individual elements and organic carbon (TOC). The TOC concentrations of Lake Sentani sediment are highly variable (3–22% dwt) and range from values typical for oligotrophic tropical lakes like Lake Towuti (2–3.5%) to eutrophic ones like Lake Maninjau (~22%) (Henny and Nomosatryo 2012; Vuillemin et al. 2016). Despite this high variability, organic matter concentrations are sufficiently high to fuel abundant microbial respiration and therefore diagenetic processes in all samples.

Calcium-bearing sediments are delivered to the lake from limestone in the catchment areas located to the southwest of the lake, bordering sub-basins 1 and 2. Production of biogenic Ca-containing minerals by calcareous plankton does not seem to play a major role as carbonates are only found in five smear slide samples (Fig. 4c). The distribution of Ca in the sediment (Fig. 3) correlates well with the smear slide data (Fig. 4c) and catchment lithology (Fig. 1b). The strong influence of catchment geology on Ca distribution is also corroborated by the distribution map of the Ca/Ti ratio (Fig. 8) showing highest values in sub-basin 2 around the Hendo sub-catchment, which is mainly composed of carbonate rocks. Slightly higher amounts of Ca and Ti in the northwestern corner of sub-basin 1 (Fig. 3) seems to originate from the basalts that make up most of the Dogefu catchment (Fig. 1a).

River samples have relatively high amounts of Si (Fig. 3), whereas lake samples show some minor

Fig. 8 Distribution of selected element ratios of sediment from river mouth and lake samples



variations in Si but no distinct distribution pattern. The Si/Ti ratio (Fig. 8) does show a strong enrichment towards the deepest part of sub-basin 4 (Fig. 8), which broadly correlates with a higher percentage of diatoms among the siliceous sediment constituents. However, in sub-basin 1 the silica fraction is also dominated by diatoms (Fig. 4), but the Si/Ti element ratio shows the opposite pattern of sub-basin 4. The very low Si/Ti ratios in sub-basin 1 are most probably caused by higher amounts of Ti in these sediments, which are higher than anywhere else in the lake.

Generally, the distribution of Si/Ti (Fig. 8) matches the distribution of diatoms in lake Sentani (Fig. 4a). Near-shore samples contain up to ~60% detrital Si, it appears that the input of Si-bearing minerals from rivers is equal to or even dwarfed by higher biogenic Si concentrations in the deeper basins. Although no data are available on the hydrodynamics in Lake Sentani, we speculate that sediment focusing can increase diatom frustule concentrations in the deepest parts of sub-basin 4, and perhaps 1 as well.

The delivery of Ca, which is almost exclusively derived from the catchment, the rivers do not seem to have much influence on sediment composition, matches the occurrence of carbonate rock fragments.

There is also no increase in the percentage of sand at the river mouths, despite all river samples having a higher sand content (Fig. 6).

Particularly in lake sediments with ultramafic catchment geology, iron concentrations are generally high and play an important role in biogeochemical processes (Costa et al. 2015; Morlock et al. 2019; Sheppard et al. 2019). An interesting observation are the elevated concentrations of monosulfide minerals (AVS fraction) in samples from rivers that drain ultramafic catchment areas (Fig. 5a). In all other samples from both rivers and the lake itself, AVS was present only in trace amounts and the CRS fraction, containing mostly pyrite, dominates the reduced inorganic sulfur species. With the exception of sub-basin 1, overall pyrite distribution showed a weak correlation with water depth. This follows the general observation that microbial sulfate reduction, the main producer of hydrogen sulfide, only occurs under reducing conditions (Widdel 1988) and therefore preferentially below the oxycline. However, oxygen penetration into the sediment is expected to be in the range of only a few mm, allowing for sulfate reduction throughout the lake's sediment. Depending on the availability of suitable metal ions, the produced hydrogen sulfide precipitates as metal sulfides. Given that iron is the most

abundant metal ion in most sedimentary systems, pyrite is the most likely end product (Berner 1984), which is also the case in Lake Sentani, as pyrite is the only reduced sulfur species detected by XRD (Fig. 5b). Sulfate concentrations in Lake Sentani are around 2 mg L^{-1} (data not shown), which is less than one thousandth as concentrated as in seawater. But even in freshwater lakes with lower sulfate concentrations, e.g. ferruginous lakes like Lake Matano or Towuti (Crowe et al. 2014; Vuillemin et al. 2016), production of hydrogen sulfide and therefore pyritization takes place, albeit on a very low level (Vuillemin et al. 2016; Friese et al. 2021). The distribution maps of TOC, Fe and S (Fig. 3) do not show a uniform pattern and in the PCA of the three clusters the vectors for these three elements show a different orientation in each cluster (Fig. 7a). The sample from the Simboro channel reveals highest sedimentary pyrite concentrations (Fig. 5a) as well as elevated concentrations of TOC and S, (Fig. 3) which we interpret as a strong indication for elevated rates of sulfate reduction in this area. However, the low concentration of sulfate in the lake water limits the overall rate of sulfate reduction, which severely reduces the quantitative importance of sulfide minerals as a sink for iron and manganese.

Geochemical characteristics of each basin

Due to the lake's peculiar shape and the highly diverse catchment, it is necessary to not simply consider the overall characteristics of the sediments but also on the level of the individual sub-basins. The daily strong winds keep the epilimnion well mixed and the basins share a common surface water chemistry (data not shown), but due to the highly diverse catchment geology each sub-basin receives a different sedimentary input. Given the steep slopes of the deep basins we argue that the water columns of at least sub-basins 1 and 4 remain well stratified throughout the year with little chances of complete overturn, although it cannot be completely ruled out, given the lake's relatively small size.

In westernmost sub-basin 1 there are two peninsulas with steep slopes on the north-eastern shore that reach far into the sub-basin (Fig. 1a). Mass wasting and direct runoff from the slope could be a possible supply mechanism for significant amounts of terrestrial material to the lake (Trescases 1973; Hasberg

et al. 2019), and in this case almost to the center of the basin. Input through rivers seems to be small and only seasonal in this sub-basin (Table 1). However, given the relatively high clay content in the southern part of the sub-basin and the dominance of silt in the north, particularly around the two peninsulas, plus very low sand content throughout sub-basin 1, and the very dense vegetation cover that provides effective protection against erosion, mass wasting also does not seem to be quantitatively important, but cannot be ruled out. Moreover, the two peninsulas have a mafic bedrock geology, but the sediments around them do not show elevated amounts of Fe, which also argues against a significant sediment input from the peninsulas. Instead, the sediment composition with higher amounts of Al, K, and Ti could rather be the result of the deposition of clays and silt that originate from chemical weathering of limestone and argillaceous sedimentary rocks from the southern part of catchment.

Due its significant water depth of 42 m, sub-basin 1 has a geochemical signature similar to the other deep sub-basin 4, despite all sites being relatively close to land. The rivers that drain into this sub-basin have relatively small discharge rates (Table 1) and some might only have water during rainy season (Handoko et al. 2014). The steep morphology in the north of the sub-basin suggests that eroded material could easily be mobilized and transported quickly by rivers, mass wasting or direct runoff from the slope. However, our data show that this is in fact not the case, as the sediments in sub-basin 1 has a more siliciclastic signature whereas the catchment in the north has a mafic composition. Literature data about the rivers are sparse and do not cover all rivers, access to the area is difficult and we were not able to sample all rivers draining into this basin, so there might be a slight mismatch between river input and sediment chemistry in our study.

The long and shallow Simboro channel between sub-basins 1 and 2 is a very efficient sediment trap that effectively isolates sub-basin 1 from the rest of the lake. The channel has a depth of about 4 m and is suspected to become even shallower in the future due to sediment deposition caused by the abundant water plants that act as efficient sediment traps (Kementarian Lingkungan Hidup Republik Indonesia 2011). A peculiar phenomenon is the strong enrichment of TOC and S in the middle of the channel (Fig. 3). The

high TOC concentration in the channel is most probably caused by an accumulation of decaying aquatic plants and the elevated S concentrations indicate enhanced sulfate reduction fueled by organic matter degradation, which is further corroborated by the high pyrite concentrations (Fig. 5).

The relatively flat topography around sub-basin 2 continues inside the lake. Sub-basin 2 is the shallowest of the four basins with a maximum depth of about 12 m. It is the only sub-basin with a fully oxygenated water column and hence, aerobic processes at the sediment–water interface. We did not measure how far oxygen penetrates into the sediment but based on our experiences from other oligotrophic lakes in Indonesia and literature data (Corzo et al. 2018), we assume that penetration depth is much less than 5 mm. Still, even with such a thin oxygenated surface layer, a significant part of the sedimentary organic matter will be degraded aerobically because aerobic degradation is much faster (Kristensen et al. 1995), decreasing the overall concentration of organic matter in deeper anoxic layers and increasing the fraction of more recalcitrant material (Westrich and Berner 1984). The diverse lithology of the different catchments is partially reflected in the element composition (Fig. 3) and the clustering results (Fig. 7). Calcium shows a very strong enrichment along the southern end of the basin (Fig. 3) and so does the Ca/Ti ratio (Fig. 8), reflecting the carbonate-rich geology of the catchment.

The geochemical characteristics of the sediment in sub-basin 3 lead to rather peculiar results of the clustering analysis. While samples from the deep lake cluster C3 are found in shallow water, the shallow lake cluster C2 occupies the deep center of the basin. This might be caused by the fact that oxygen concentrations in sub-basin 3 barely reach depletion at the SWI, providing the potential for repeated oxygenation–reduction cycles that can promote mineral precipitation. Those samples from sub-basin 3 that fall in cluster C2 show negative PC1 values (Fig. 7b), indicating a positive correlation with Fe and Mn and partially S. Those samples that fall into cluster C3 have a positive PC1 score, revealing a positive correlation with elements indicative of detrital input from siliciclastic rocks. Elemental distributions (Fig. 3) and element ratios (Fig. 8) do not show any particular enrichments in this basin, with the exception of a decreasing north–south gradient of the Fe/Ti ratio,

most probably caused by the greater input of Fe from the Cycloops Mountains in the north.

Samples from sub-basin 4 fall almost entirely into Cluster C3, most probably due to greater water depth and the strong riverine input of Fe and Mn from the mafic and ultramafic catchment on the northern shore. There are 3 rivers with a total discharge of $0.9 \text{ m}^3 \text{ s}^{-1}$ draining into sub-basin 4, but only one river with $0.36 \text{ m}^3 \text{ s}^{-1}$ into sub-basin 3 (Table 1). The Yabawi river, which drains the Yakembeng sub-catchment enters Lake Sentani close to the sill between the two basins so we cannot assign it to either basin. A peculiar feature of sub-basin 4 are the enrichments of Fe and Mn (Fig. 3), although in different locations for each element. While highest amounts of Mn and Mn/Ti ratios are found in the deepest part of the sub-basin, Fe show a general decrease from north to south and no correlation with water depth. The Fe/Ti ratio (Fig. 8) however, reveals a distinct minimum at the deepest part of the sub-basin and a gradual increase towards the southern end of the sub-basin where the only outlet is located. We interpret this pattern as a combination of different processes. A strong riverine input of Fe from the ultramafic catchments in the north of the lake leads to higher amounts of Fe and Fe/Ti ratios right along the river mouths of the northern shoreline and in near-shore locations in deeper water, given the very steep slope in this area. It is surprising that only Fe shows such a distribution pattern and not Mn, considering that ultramafic rocks also contain considerable amounts of Mn. Here it seems that Fe behaves more like a detrital element, whereas Mn shows the behavior of a redox-sensitive element. We can only speculate about the reasons, detailed mineralogical studies that are beyond the scope of this study might be able to shed light into this phenomenon.

The deepest part of sub-basin 4 has fully reducing conditions, yet it reveals high amounts of Mn as well as highest Mn/Ti ratios. Under such conditions Mn should be reduced and highly soluble. At first glance the massive enrichment of Mn in the deepest part of sub-basin 4 suggests at least occasional complete overturning, as oxidation of the bottom water would lead to oxidation and precipitation of dissolved Mn. However, the lack of concomitant iron enrichments argues against overturning: Iron is also abundant in Lake Sentani and has similar redox behavior as Mn. It remains questionable whether the faster oxidation and dissolution kinetics of Fe in comparison to Mn (Martin 2005) could explain

the specific enrichment of Mn but not Fe in the deepest part of sub-basin 4. Unfortunately, our XRD results (Fig. 5b) do not reveal any Mn-rich mineral in sub-basin 4, so we do not know in which mineral the Mn is bound.

Transport processes also do not seem to play a major role in sub-basin 4 as there are no obvious patterns in the distribution of the different size classes (Fig. 6). The PCA of Cluster C3 shows an almost perfect correlation between location and PC1, the most negative PC1 values, strongly correlating with Mn, are found in the center of the basin, and steadily increase towards the south (Fig. 7b), indicating a correlation with mainly Al and Ti. This is not surprising, given the fact that both the eastern and western shores of this narrow sub-basin are bounded by clay- and siltstones and alluvial fan deposit (Fig. 1b). Although these rocks have a rather diverse geochemical signature, what they have in common is the different composition in comparison to ultramafic rocks in the north. Moreover, the narrow and shallow shape of the southern end of the sub-basin allows for complete mixing and resuspension of material during storm events at least in this part. Such events probably remove most small-scale differences between the different sediment sources.

The recent study of Nomosatryo et al. (2021) presents geochemical depth profiles of sediment cores from each sub-basin, showing clear compositional differences between sites and with depth, and each sub-basin shows distinctly different trends. The present study focuses just on the sediment surface, albeit in higher spatial resolution. The geochemical data presented in both studies highlight the fact that studies addressing climate or hydrological variations based on lacustrine sediment records should use great care to distinguish between site-specific characteristics, which can be influenced by a great variety of processes, and variations caused by regional changes in climate or hydrology.

Conclusions

The overall patterns in geochemical composition between the different sub-basins and within each individual sub-basin are mainly caused by a combination of catchment geology and redox chemistry. Catchment geology seems to be the most important factor, the most obvious examples are the relative enrichment

of iron, manganese and mafic minerals in those parts of the lake that are bounded by ultramafic catchment, as well as the presence of carbonates only in areas with a connection to catchments that are dominated by either carbonate rocks or basalts. The effects of transport processes appear to be only minor. The lake itself has an almost bimodal distribution of clay and silt that does not correlate with any other parameter, and sand only makes up a minor proportion of the total sediment and is very evenly distributed across the lake, despite having much higher concentrations in the rivers. Although we do see a clear influence of catchment geology on lake sediment composition, the rivers do not seem to leave a major imprint on the lake, neither with regard to grain size distribution nor chemistry. Mass wasting or direct runoff does have an influence on sediment chemistry, one example is the change in sediment composition in the southern part of sub-basin 4, where the compositional change correlates with the more siliciclastic catchment geology on both sides of this part of the sub-basin. However,

the fact that there is no increase in grain size argues against mass wasting, so the final verdict about the influence on mass wasting on overall sediment composition is still out.

Acknowledgements The authors would like to thank director and staff of Research Center for Limnology-LIPI (BRIN) for the general and technical support. Pugh Sujarta, Henderite Ohee, Ela Korwa, (Cendrawasih University, Papua) and the late Herry Kopalit (University of Papua, Manokwari) managed field work. Axel Kitte, Brian Brademann, Nikolai Klitscher (GFZ Potsdam) are thanked for assistance in the lab and in the field. Grain size analysis was carried out by Gunnar Pruß (Section Geomorphology, GFZ Potsdam), Dyke Scheidemann (AWI Potsdam) provided TOC data. Anja Schleicher (Section Inorganic and Isotope Geochemistry, GFZ Potsdam) provided XRD data.

Funding Open Access funding enabled and organized by Projekt DEAL. SN was financially supported by the Program for Research and Innovation in Science and Technology (RISET-Pro, World Bank Loan No. 8245-ID)—Ministry of Research, Technology and Higher Education, Republic of Indonesia.

Open Access This article is licensed under a Creative Commons Attribution 4.0 International License, which permits use, sharing, adaptation, distribution and reproduction in any medium or format, as long as you give appropriate credit to the original author(s) and the source, provide a link to the Creative Commons licence, and indicate if changes were made. The images or other third party material in this article are included in the article's Creative Commons licence, unless indicated

otherwise in a credit line to the material. If material is not included in the article's Creative Commons licence and your intended use is not permitted by statutory regulation or exceeds the permitted use, you will need to obtain permission directly from the copyright holder. To view a copy of this licence, visit <http://creativecommons.org/licenses/by/4.0/>.

References

- Bauer KW, Byrne JM, Kenward P, Simister RL, Michiels CC, Friese A, Vuillemin A, Henny C, Nomosatryo S, Kallmeyer J, Kappler A, Smit MA, Francois R, Crowe SA (2020) Magnetite biomineralization in ferruginous waters and early Earth evolution. *Earth Planet Sc Lett* 549:116495
- Berner RA (1984) Sedimentary pyrite formation: an update. *Geochim Cosmochim Acta* 48:605–615
- Boehrer B, Schultze M (2008) Stratification of lakes. *Rev Geophys* 46:1–27
- Bungkang Y, Soemarno AD, Bisri M (2014) Sentani watershed erosion potential study and suspended solid distribution (TSS) in connection with lake silting. *IOSR J Environ Sci Toxicol Food Technol* 8:36–43
- Canfield DE, Raiswell R, Westrich JT, Reaves CM, Berner RA (1986) The use of chromium reduction in the analysis of reduced inorganic sulfur compounds in sediments and shales. *Chem Geol* 54:149–155
- Capone DG, Kiene RP (1988) Comparison of microbial dynamics in marine and freshwater sediments: contrasts in anaerobic carbon catabolism. *Limnol Oceanogr* 33:725–749
- Cline JD (1969) Spectrophotometric determination of hydrogen sulfide in natural waters. *Limnol Oceanogr* 14:454–458
- Corzo A, Jiménez-Arias JL, Torres E, García-Robledo E, Lara M, Papaspyrou S (2018) Biogeochemical changes at the sediment–water interface during redox transitions in an acidic reservoir: exchange of protons, acidity and electron donors and acceptors. *Biogeochemistry* 139:241–260
- Costa KM, Russell JM, Vogel H, Bijaksana S (2015) Hydrological connectivity and mixing of Lake Towuti, Indonesia in response to paleoclimatic changes over the last 60,000 years. *Palaeogeogr Palaeoclimatol Palaeoecol* 417:467–475
- Crowe SA, O'Neill AH, Katsev S, Hehanussa P, Haffner GD, Sundby B, Mucci A, Fowle DA (2008) The biogeochemistry of tropical lakes: a case study from Lake Matano, Indonesia. *Limnol Oceanogr* 53:319–331
- Crowe SA, Paris G, Katsev S, Jones CA, Kim ST, Zerkle AL, Nomosatryo S, Fowle DA, Adkins JF, Sessions AL, Farquhar J, Canfield DE (2014) Sulfate was a trace constituent of Archean seawater. *Science* 346:735–739
- De Crop W, Verschuren D (2019) Determining patterns of stratification and mixing in tropical crater lakes through intermittent water-column profiling: a case study in western Uganda. *J Afr Earth Sci* 153:17–30
- Dietze E, Hartmann K, Diekmann B, Ijmker J, Lehmkuhl F, Opitz S, Stauch G, Wünnemann B, Borchers A (2012) An end-member algorithm for deciphering modern detrital processes from lake sediments of Lake Donggi Cona, NE Tibetan Plateau, China. *Sediment Geol* 243:169–180
- Escobar J, Serna Y, Hoyos N, Velez MI, Correa-Metrio A (2020) Why we need more paleolimnology studies in the tropics. *J Paleolimnol* 64:47–53
- Fauzi M, Rispiningtati R, Hendrawan AP (2014) Kajian kemampuan maksimum danau Sentani dalam mereduksi banjir di DAS Sentani. *Jurnal Teknik Pengairan* 5:42–53
- Fredrickson JK, Zachara JM, Kennedy DW, Dong H, Onstott TC, Hinman NW, Li SM (1998) Biogenic iron mineralization accompanying the dissimilatory reduction of hydrous ferric oxide by a groundwater bacterium. *Geochim Cosmochim Acta* 62:3239–3257
- Friese A, Bauer K, Glombitza C, Ordoñez L, Ariztegui D, Heuer VB, Vuillemin A, Henny C, Nomosatryo S, Simister R, Wagner D, Bijaksana S, Vogel H, Melles M, Russell JM, Crowe SA, Kallmeyer J (2021) Organic matter mineralization in modern and ancient ferruginous sediments. *Nat Commun* 12:1–9
- Froehlich PN, Klinkhammer GP, Bender ML, Luedke NA, Heath GR, Cullen D, Dauphin P, Hammond D, Hartman B, Maynard V (1979) Early oxidation of organic matter in pelagic sediments of the eastern equatorial Atlantic: suboxic diagenesis. *Geochim Cosmochim Acta* 43:1075–1090
- Hammer Ø, Harper DAT, Ryan PD (2001) PAST: paleontological statistics software package for education for education and data analysis. *Palaeontol Electron* 4:9
- Handoko U, Suryono T, Sadi NH (2014) Karakteristik fisika-kimia sungai inlet-outlet danau Sentani Papua. In: Subehi L, Haryani GS, Henny C, Wibowo H (eds) *Prosiding Seminar Nasional Limnologi VII Tahun 2014*. Gedung APCE, Cibinong Science Centre-Botanical Garden, pp 226–236
- Hasberg AKM, Bijaksana S, Held P, Just J, Melles M, Morlock MA, Opitz S (2019) Modern sedimentation processes in Lake Towuti, Indonesia, revealed by the composition of surface sediments. *Sedimentology* 66:675–698
- Henny C, Nomosatryo S (2012) Dinamika sulfida di danau maninjau: implikasi terhadap pelepasan fosfat di lapisan hipolimnion. *Limnotek* 19:91–106
- Holmer M, Storkholm P (2001) Sulphate reduction and sulphur cycling in lake sediments: a review. *Freshw Biol* 46:431–451
- Husein S, Syahputra R, Nukman M, Setiawan NI, Wicaksono DT, Nugroho W (2018) Morphotectonic and orogenic uplift of Cyclops Mountains, Papua. *Proceedings Pekan Ilmiah Tahunan IAGI*, 2018
- Hutchinson GE (1957) *A treatise on limnology; geography, physics and chemistry*. Wiley, New York
- Indrayani E, Nitimulyo KH, Hadisusanto S (2015a) Peta batimetri Danau Sentani Papua. *Depik* 4:116–120
- Indrayani E, Nitimulyo KH, Hadisusanto S, Rustadi R (2015b) Analisis kandungan nitrogen, fosfor dan karbon organik di Danau Sentani—Papua. *Jurnal Manusia Dan Lingkungan* 22:217–225
- Kallmeyer J, Ferdelman TG, Weber A, Fossing H, Jørgensen BB (2004) A cold chromium distillation procedure for radiolabeled sulfide applied to sulfate reduction measurements. *Limnol Oceanogr Methods* 2:171–180

- Katsev S, Verburg P, Llíros M, Minor EC, Kruger BR, Li J (2017) Tropical meromictic lakes: specifics of meromixis and case studies of lakes Tanganyika, Malawi, and Matano. In: Gulati R, Zadereev E, Degermendzhi A (eds) Ecology of meromictic lakes. *Ecol Stud* 228:277–323
- Kementerian Lingkungan Hidup Republik Indonesia (2011) Profil 15 Danau Prioritas Nasional. Kementerian Lingkungan Hidup, Jakarta
- Kristensen E, Ahmed SI, Devol AH (1995) Aerobic and anaerobic decomposition of organic matter in marine sediment: which is fastest? *Limnol Oceanogr* 40:1430–1437
- Last WM, Smol JP (2001) Basin analysis, coring, and chronological techniques. Springer, Dordrecht
- Lewis WMLJ (1987) Tropical limnology. *Annu Rev Ecol Evol Syst* 18:159–184
- Liu Z, Wang H, Hantoro WS, Sathiamurthy E, Colin C, Zhao Y, Li J (2012) Climatic and tectonic controls on chemical weathering in tropical Southeast Asia (Malay Peninsula, Borneo, and Sumatra). *Chem Geol* 291:1–12
- Luther GWI (1987) Pyrite oxidation and reduction: molecular orbital theory considerations. *Geochim Cosmochim Acta* 51:3193–3199
- Mantiri SY (2016) Variasi nilai frekuensi, akumulasi energi dan parameter seismik secara temporal di wilayah Jayapura periode 1965–2014. *Sains* 16:35–43
- Martin ST (2005) Precipitation and dissolution of iron and manganese oxides. *Environ Catal* 1:61–82
- Morlock MA, Vogel H, Nigg V, Ordon L, Hasberg AKM, Melles M, Russell JM, Bijaksana S (2019) Climatic and tectonic controls on source-to-sink processes in the tropical, ultramafic catchment of Lake Towuti, Indonesia. *J Paleolimnol* 61:279–295
- Nomosatryo S, Tjallingii R, Schleicher AM, Boli P, Henny C, Wagner D, Kallmeyer J (2021) Geochemical characteristics of sediment in tropical lake sentani, indonesia, are influenced by spatial differences in catchment geology and water column stratification. *Front Earth Sci* 9:350
- Raiswell R, Canfield DE (2012) The iron biogeochemical cycle past and present. *Geochem Perspect* 1:1–232
- Roland FAE, Darchambeau F, Borges AV, Morana C, Thandrup B, De BL, Crowe SA (2017) Denitrification, anaerobic ammonium oxidation, and dissimilatory nitrate reduction to ammonium in an East African Great Lake (Lake Kivu). *Limnol Oceanogr* 63:687–701
- Sadi NH (2014) Laporan Eksekutif: Karakterisasi hidroklimatologi dan penetapan status sumber daya perairan darat di danau Sentani, Papua. Pusat Penelitian Limnologi-Lembaga Ilmu Pengetahuan Indonesia (LIPI), Cibinong
- Santschi P, Höhener P, Benoit G, Buchholtz-ten BM (1990) Chemical processes at the sediment-water interface. *Mar Chem* 30:269–315
- Sartimbul A, Mujiadi H, Rahardjo SSP, Suryono A (2015) Analisis kapasitas tampungan danau sentani untuk mengetahui fungsi detensi dan retensi tampungan. *Limnotek* 22:208–226
- Sheppard RY, Milliken RE, Russell JM, Dyar MD, Sklute EC, Vogel H, Melles M, Bijaksana S, Morlock MA, Hasberg AKM (2019) Characterization of iron in Lake Towuti sediment. *Chem Geol* 512:11–30
- Stallard RF (1998) Terrestrial sedimentation and the carbon cycle: coupling weathering and erosion to carbon burial. *Glob Biogeochem Cycles* 12:231–257
- Stallard RF, Edmond JM (1983) Geochemistry of the Amazon: 2. The influence of geology and weathering environment on the dissolved load. *J Geophys Res* 88:9671–9688
- Suwarno N, Noya Y (1995) Geological map of The Jayapura (Peg. Cycloops) Quadrangle, Irian Jaya. Indonesia Geological Research and Development Centre (Pusat Penelitian dan Pengembangan Geologi), Bandung
- Tappin AR (2007) Freshwater biodiversity of New Guinea. In-Stream. Australia-New Guinea Fishes Association Queensland Inc.: pp 1–62
- Trescases JJ (1973) Weathering and geochemical behaviour of the elements of ultramafic rocks in New Caledonia. Bureau Miner Resour Geol Geophys Canberra 141:149–161
- van 't Hoff Schröder JT, Held P, Opitz S, Wagner B, Reicherter K, Melles M (2016) Modern sedimentation processes in Laguna de Medina, southern Spain, derived from lake surface sediment and catchment soil samples. *J Limnol* 76:103–115
- Vogel H, Wessels M, Albrecht C, Stich HB, Wagner B (2010) Spatial variability of recent sedimentation in Lake Ohrid (Albania/Macedonia). *Biogeosciences* 7:3333–3342
- Vuillemin A, Friese A, Alawi M, Henny C, Nomosatryo S, Wagner D, Crowe SA, Kallmeyer J (2016) Geomicrobiological features of ferruginous sediments from Lake Towuti, Indonesia. *Front Microbiol* 7:1007
- Vuillemin A, Wirth R, Kemnitz H, Schleicher AM, Friese A, Bauer KW, Simister R, Nomosatryo S, Ordoñez L, Ariztegui D, Henny C, Crowe SA, Benning LG, Kallmeyer J, Russell JM, Bijaksana S, Vogel H, The Towuti Drilling Project Science Team (2019) Formation of diagenetic siderite in modern ferruginous sediments. *Geology* 47:540–544
- Vuillemin A, Friese A, Wirth R, Schuessler JA, Schleicher AM, Kemnitz H, Lücke A, Bauer KW, Nomosatryo S, Von BF, Simister R, Ordoñez LG, Ariztegui D, Henny C, Russell JM, Bijaksana S, Vogel H, Crowe SA, Kallmeyer J (2020) Vivianite formation in ferruginous sediments from Lake Towuti, Indonesia. *Biogeosciences* 17:1955–1973
- Wennrich V, Francke A, Dehnert A, Juschus O, Leipe T, Vogt C, Brigham-Grette J, Minyuk PS, Melles M, El'gygytgyn SP (2013) Modern sedimentation patterns in Lake El'gygytgyn, NE Russia, derived from surface sediment and inlet streams samples. *Clim past* 9:135–148
- Weltje GJ, Tjallingii R (2008) Calibration of XRF core scanners for quantitative geochemical logging of sediment cores: theory and application. *Earth Planet Sci Lett* 274:423–438
- Weltje G, Bloemsma M, Tjallingii R, Heslop D, Röhl U, Croudace I (2015) Prediction of geochemical composition from xrf core scanner data: a new multivariate approach including automatic selection of calibration samples and quantification of uncertainties. In:

- Croudace I, Rothwell R (eds) Micro-XRF studies of sediment cores. *Dev Paleoenviron Res* 17, pp 507–534
- Westrich JT, Berner RA (1984) The role of sedimentary organic matter in bacterial sulfate reduction: the G model tested 1. *Limnol Oceanogr* 29:236–249
- Widdel F (1988) Microbiology and ecology of sulfate- and sulfur-reducing bacteria. In: Zehnder AJB (ed) *Biology of anaerobic microorganism*. Wiley, New York, pp 469–585
- Yuretich RF (1979) Modern sediments and sedimentary processes in Lake Rudolf (Lake Turkana) eastern Rift Valley, Kenya. *Sedimentology* 26:313–331
- Zegeye A, Bonneville S, Benning LG, Sturm A, Fowle DA, Jones CA, Canfield DE, Ruby C, MacLean LC, Nomosatryo S, Crowe SA, Poulton SW (2012) Green rust formation controls nutrient availability in a ferruginous water column. *Geology* 40:599–602

Publisher's Note Springer Nature remains neutral with regard to jurisdictional claims in published maps and institutional affiliations.